

Maximizing Energy Output of Explosively-Driven Ferromagnetic Generators

Contents

1. Introduction	384
2. Experiments	385
3. Results and Discussions	385
3.1. Cylinder-type FMGs	385
3.2. Voltage	386
3.3. Energy	388
3.4. Annulus-type FMGs	390
4. Conclusions	390

Abstract

We designed two different types of explosively-driven ferromagnetic generators based on NdFeB magnets; cylinder- and annulus-types. We investigated the output characteristics of those generators while varying design features; length and diameter of magnets, pitch or turns of generator coils, and inductance of loads. We performed hydrodynamic simulations extensively for shockwave propagation in magnets for both types of generators. Based on experimental and calculational results, we optimized the designs to maximize the energy output. The maximum energy obtained was 0.9 J with an energy conversion efficiency of 6.7 % for the cylinder-type generator with magnets of 50 mm in diameter and 25 mm in length, and 1.5 J with an efficiency of 9.4 % for the annulus-type generators with magnets of 50 mm in diameter and 40 mm in length.

1. Introduction

Ferromagnetic generators (FMGs) are devices which convert magnetic energy into electrical energy by demagnetization of ferromagnets. FMGs are simple in design, stable in performance, compact in size, and autonomous in operation. Because of these advantages, FMGs have been studied extensively as a compact autonomous pulsed-power source by Kristiansen [1], Shkuratov et al. [2,3], Lee et al. [4], Choi et al. [5].

In FMGs, ferromagnets are demagnetized by shock loading either from impact of high-speed flyers or from detonation of high explosives. Royce [6] showed experimentally that the shock-induced demagnetization of iron took place abruptly at about 13 GPa. This is caused by phase transformation of iron from BCC α -phase to FCC γ -phase [7]. In

Graham’s experiments [8], demagnetization of Invar (36 Ni/ 64 Fe) and Silectron (3 Ni/ 97 Fe) increased gradually with increasing shock pressure. However, demagnetization of NdFeB has not been fully studied yet. In this study, complete demagnetization of NdFeB was assumed occur at 13 GPa, demagnetization pressure of iron, because of lack of information. Though, it is suspected that the pressure should be lower than 13 GPa, and that considerable demagnetization should occur below that pressure.

The objectives of this study are to investigate the effect of design features on outputs of FMGs based on NdFeB magnets and to optimize designs of cylinder- and annulus-type FMGs based on results obtained from series of experimental and hydrodynamic calculations.

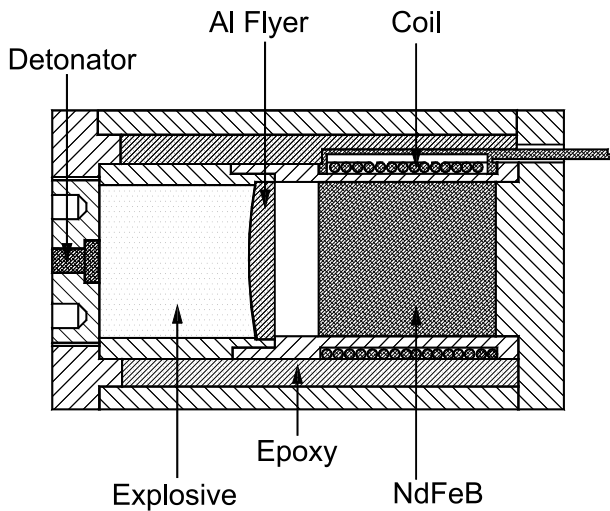


Fig. 1. Schematic of the cylinder-type FMG.

Table 1. Properties of NdFeB magnets

property	density (g/cm ³)	B (T)	Hc (A/m)	BHmax (T A/m)
value	7.43	1.2	890,000	270,000

2. Experiments

Figure 1 shows the schematic design of the cylinder-type FMG. The shock generator, an explosive pellet and an aluminum flyer plate, was designed to generate a plane shockwave of 30 GPa at the impact surface of the magnet. For a magnet of 25 mm in diameter, the thickness of the flyer plate 3.5 mm on axis and 2.5 mm on edge. An experimental explosive whose detonation properties were very similar to those of LX-14 [9] was used to accelerate the flyer plate. The weight of the explosive pellet was 19.6 g, and its thickness was 21.5 mm on axis and 22.5 mm on edge. The details of the shock generator design were adjusted according to the magnet diameter. The diameter and length of magnets were varied from 25 to 50 mm, and from 20 to 40 mm, respectively. The properties of NdFeB magnets, manufactured by Daeho Magnets, Seoul, Korea, are listed in Table 1.

The generator coil was fabricated by using an enameled copper wire of 1 mm in diameter. The pitch of the coil was varied from 0.5 to 3 mm. The values of inductance and resistance of coils and loads measured at a frequency of 100 kHz are listed together with experimental results in Table 2.

Figure 2 shows the annulus-type FMG. In this type of FMG, a demagnetization shock is transmitted from detonation of a cylindrical explosive charge located at the central axis of the magnet instead of using

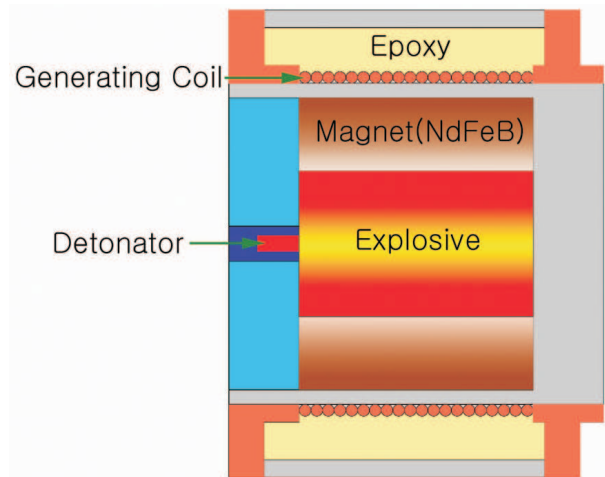


Fig. 2. Schematic of the annulus-type FMG.

a shock generator. The inside and outside diameters of an annular magnet were 25 and 50 mm, and its length was either 40 or 80 mm. The generator coil and load were fabricated by using the same materials with those of the cylinder-type FMG. Composition C-4 explosive was for convenience. The design parameters are summarized together with experimental results in Table 3.

In every test, voltage and current were recorded. Voltage was measured directly by using a high-resistance divider across the load. Current was obtained by integrating dI/dt , where I is current, from a Rogowski coil placed near the load.

3. Results and Discussions

3.1. Cylinder-type FMGs

Twenty three tests were conducted for the cylinder-type designs. Tests C1 to C14 were made by using the shock generator shown in Figure 1. To increase the duration of the shockwave, the shock generator was modified: the thickness of the aluminum flyer was increased by 1 mm and the weight of the explosive was increased accordingly. Tests C24 to C32 were done by using the modified shock generators. The test results are summarized in Table 2. Based on these results, effects of important design parameters on outputs will be discussed.

The typical voltage and current wave forms for both types of FMGs are shown in Figure 3. In Figure 3, for a cylinder-type FMG, the voltage, or dI/dt , increased very rapidly at the shockwave arrival, dropped abruptly down to a certain level, stayed for a while, and started to decay rather slowly. This abrupt drop from the peak can be attributed mainly to the effect of eddy current as discussed by Kristiansen [1]. The eddy current was generated

Table 2. Design parameters and experimental results for the cylinder-type FMGs

Test	Magnet	Coil		Load		Output		
	Diameter/ Length (mm)	Turn/ Pitch (mm)	Inductance (μH)	Inductance (μH)	Resistance (Ω)	Voltage (V)	Current (A)	Energy (J)
C1	25/40	38/1.0	10.2	10.7	0.17	202	166	0.147
C2	25/40	25/1.5	4.6	4.5	0.09	133	238	0.127
C3	25/40	19/2.0	2.7	2.7	0.05	80	–	–
C4	25/20	19/1.0	4.7	open	–	456	–	–
C5	25/40	38/1.0	10.0	open	–	441	–	–
C6	25/60	58/1.0	15.9	open	–	480	–	–
C7	25/20	19/1.0	4.4	4.4	0.09	–	251	0.139
C8	25/40	38/1.0	10.0	10.2	0.15	–	194	0.191
C9	25/60	58/1.0	16.4	16.2	0.21	–	92	0.069
C10	25/20	19/1.0	4.8	4.6	0.09	209	258	0.153
C11	25/40	38/1.0	10.8	10.0	0.15	200	170	0.145
C12	25/60	58/1.0	16.5	16.4	0.21	210	93	0.072
C13	25/20	26/0.75	9.1	4.6	0.09	189	252	0.146
C14	25/20	45/0.5	19.2	4.5	0.10	145	185	0.077
C24	25/20	18/1.1	–	9.6	0.05	242	194	0.180
C25	25/40	37/1.1	–	24.3	0.09	273	113	0.154
C26	36/20	18/1.1	–	15.0	0.06	495	215	0.348
C27	36/40	37/1.1	–	40.6	0.12	495	190	0.731
C28	50/25	18/1.1	–	22.8	0.08	901	277	0.872
C29	50/50	37/1.1	–	64.6	0.15	906	–	–
C30	25/20	18/1.1	–	9.6	0.05	253	183	0.161
C31	36/20	18/1.1	–	14.9	0.06	516	235	0.411
C32	50/25	18/1.1	–	22.1	0.07	834	286	0.902

because the shockwave moved in parallel with the magnetic flux.

3.2. Voltage

For the same pitch of 1 mm, as in Test 1 and Tests 10–12, the peak voltage was nearly constant regardless of the magnet length and the load; from 200 to 210 V. This can be explained qualitatively by assuming an ideal case, constant magnetic flux density throughout the whole magnet, as follows;

$$emf = \frac{d\Phi}{dt} = \frac{d}{dt}(BAN) = nBA \frac{d\lambda}{dt} = \frac{BA}{p} \frac{d\lambda}{dt} \quad (1)$$

where emf is electromotive force, Φ is flux, t is time, B is flux density, A is cross-sectional area, N is total turns of a coil, n is turns per unit length, λ is length of the magnet, and p is pitch of the coil. From Equation

(1), emf is expected to be inversely proportional to the pitch of a coil, and proportional to the cross-sectional area of a magnet. The initial peak voltage, then, should remain constant regardless of the magnet length if the coil pitch and magnet diameter are the same. This was manifested in Tests C4 to C6: the first peak voltage was nearly constant, about 460 V. When the pitch was increased from 1 to 2 mm as in Test C2, the peak voltage was decreased from 202 to 133 V, which can be expected from Equation (1).

In Tests C10, C13 and C14, the voltage was decreased with decreasing pitch, contrary to Equation (1). This case, however, has to be excluded in evaluating the effect of pitch on the load voltage because the inductance of the loads was not matched to that of the coils. If the inductance of the loads had been matched, the output voltage could have been

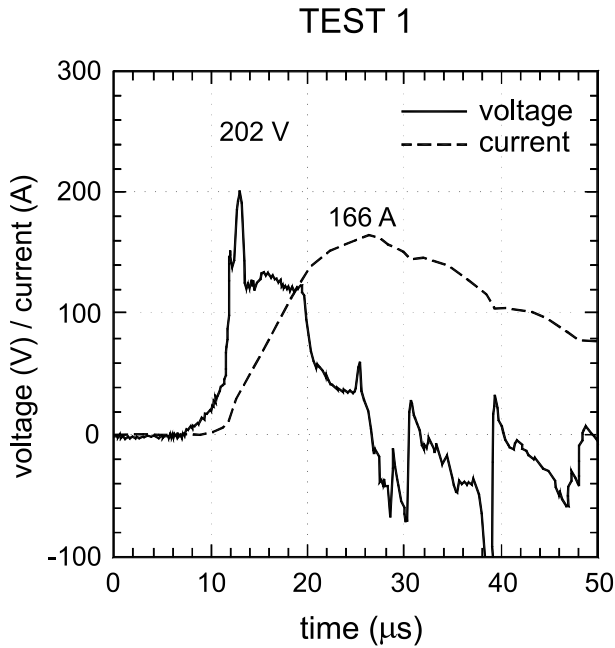


Fig. 3. Typical voltage and current waveforms for the cylinder-type FMG.

higher, judging from the other test outputs.

Results from Tests C24 to C32 showed the effect of the cross-sectional area on the peak voltage. The voltage was approximately proportional to the squared diameter, or cross-sectional area, as expected from Equation (1). The voltage in these tests was generally higher than that in Tests C1 to C14. It was because, in these tests, the design of the shock generator was modified to increase the velocity of the flyer plate, and, as a result, the velocity of the shock wave was higher.

Although it did not affect the peak voltage, the length of a magnet influenced the voltage wave form. Hydrodynamic calculations showed that the plane shockwave at the impact surface became curved owing to the expansion wave coming from sides as it propagated through the magnet, and, consequently, the wave was slowed down. The evolution of the shock front curvature and the decrease in shockwave velocity are shown in Figures 4 and 5, respectively. These results were obtained from calculations for a magnet of 25 mm in diameter and 40 mm in length impacted by an aluminum flyer of 2.83 mm in thickness at 2.1 mm/ms.

In Figure 5, the shockwave propagated into the magnet at 5.2 mm/μs at the impact surface was slowed down to 4.2 mm/μs at the axis, and 3.9 mm/μs near the edge after traveling 40 mm. These decrease in shockwave velocity resulted in the decrease in voltage in time, as expected from Equation (1).

The term A in Equation (1) is not the physical cross-sectional area of the magnet, but the surface area of the shockwave front in the magnet. They are

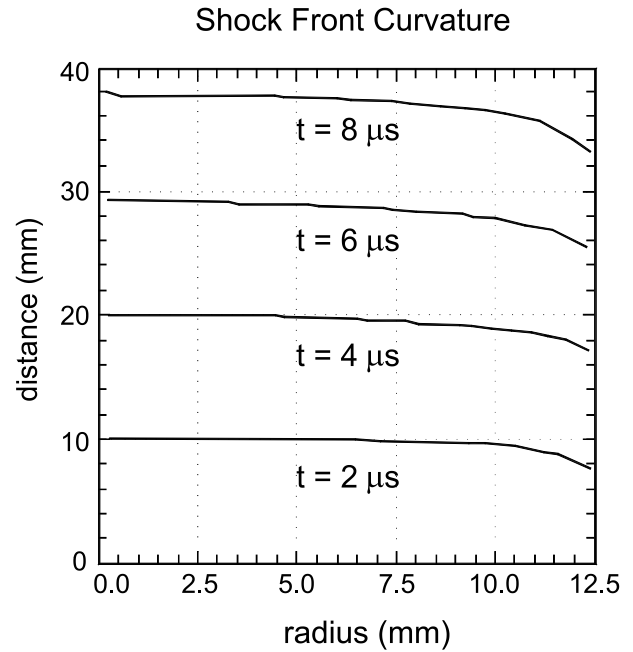


Fig. 4. Evolution of the shock front curvature.

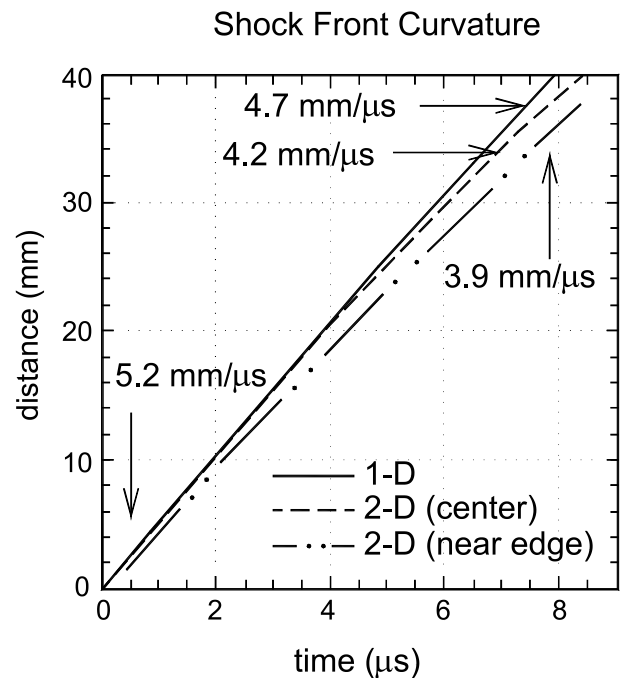


Fig. 5. Position of the shock front in the magnet.

the same only when the shockwave front is plane. To include the effect of curved front, Equation (1) is rewritten into:

$$emf = \frac{RBA}{p} \frac{d\lambda}{dt} = \frac{B}{p} \frac{d(A\lambda)}{dt} = \frac{B}{p} \frac{dV_s}{dt} \quad (2)$$

where V_s is shocked volume. Equation (2) clearly shows that the voltage is proportional to the rate of shocked volume change, dV_s/dt , assuming constant magnetic flux density. The rate of shocked volume

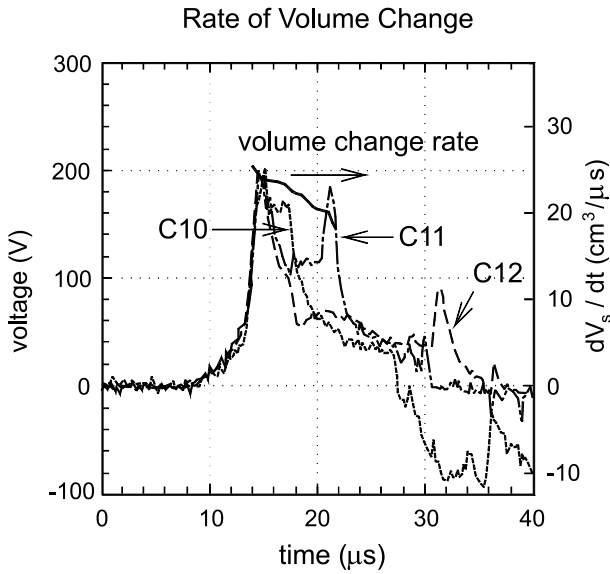


Fig. 6. Rate of volume change and voltage waveforms.

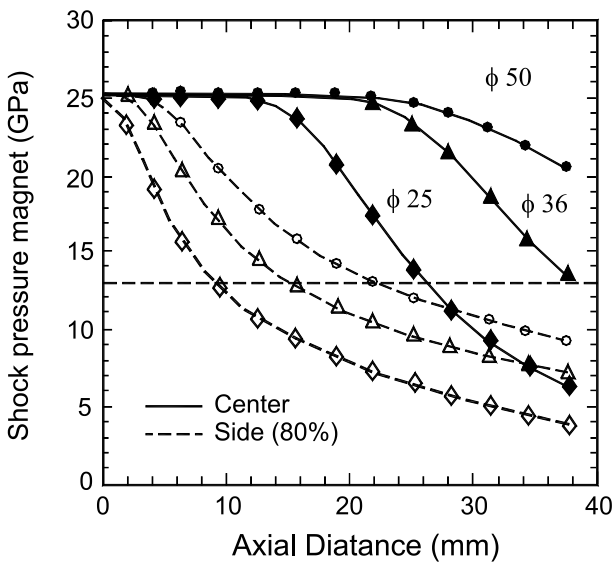


Fig. 7. Decay in shock pressure in magnets.

was calculated and compared with voltage waveforms obtained from Tests C10 to C12; magnet length of 20 mm in Test C10, 40 mm in Test C11, and 60 mm in Test C12. Figure 6 shows a good agreement between the calculated volume change rate and the voltage wave forms, considering the eddy current effect.

3.3. Energy

Comparing energy output obtained from Tests C10, C13, and C14, it can be found that the energy output was the highest for the matched load, although not conclusive because of lack of data. Results from Test C1 to 14 showed that the pitch, or the number of coil turns, did not influence the energy output when the load was matched to the generator coil. This suggests that the inductance of a generator coil has to

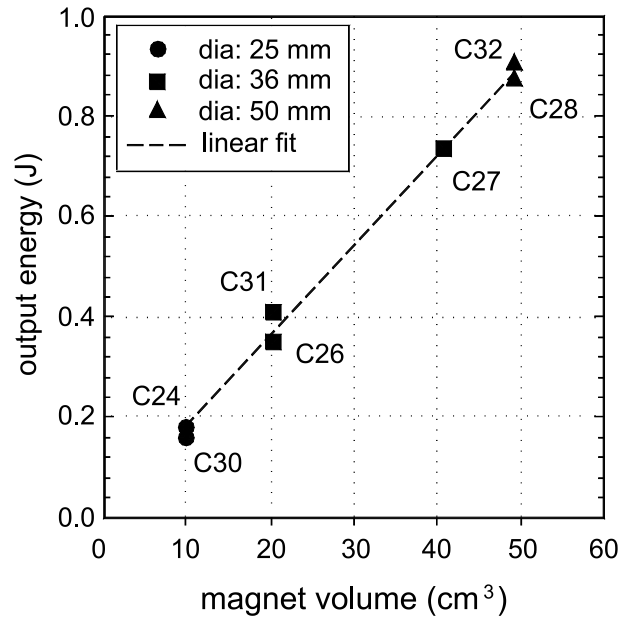


Fig. 8. Output energy as a function of magnet volume.

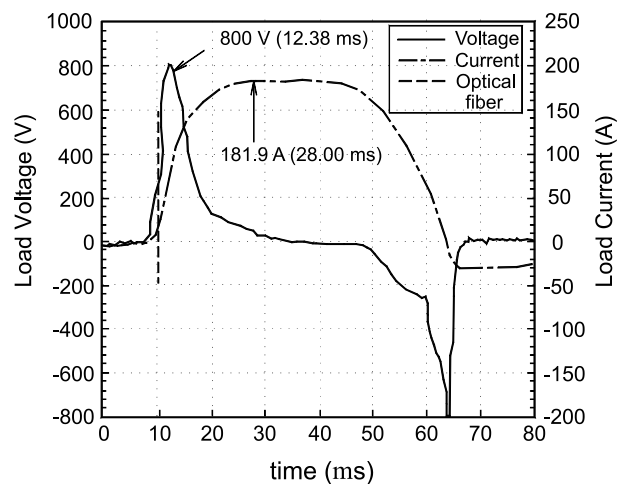


Fig. 9. Typical voltage and current waveforms for the annulus-type FMG.

be matched to that of a load to maximize the energy output of a FMG.

It could be expected that the energy output would be greater with larger magnet volume. The energy output obtained from Tests C24 to C32 confirmed this expectation. However, results from Tests C1 to C14 were completely out of the above trend. The energy output averaged for matched loads was estimated to be 0.146 J for 20 mm in magnet length, 0.153 J for 40 mm, and 0.071 J for 60 mm. Hydrodynamic calculations provided a clue for these contradicting results.

Figure 7 shows the decay in peak pressure of the shockwave propagating through magnets of 25 mm, 36 mm, and 50 mm in diameter. In Figure 7, for a magnet 25 mm in diameter, the shock pressure

Table 3. Design parameters and experimental results for the annulus-type FMGs

Test	Magnet length (mm)	Coil		Load	Output		
		Turn	Inductance (μH)		Voltage (V)	Current (A)	Energy(J)
A16	40	37	68.8	30.9 μH	> 800	181.9	0.5
A17	40	37	68.8	23.25 Ω	1672	77.4	1.75
A18	40	37	68.8	open	> 2500	–	–
A19	40	37	69.1	open	2590	–	–
A20	40	37	68.8	70 μH	1520	209.6	1.5
A22	80	76	176.7	23.25 Ω	1800	89.5	3.0
A23	80	37x2	44	23.25 Ω	1150	80	1.75

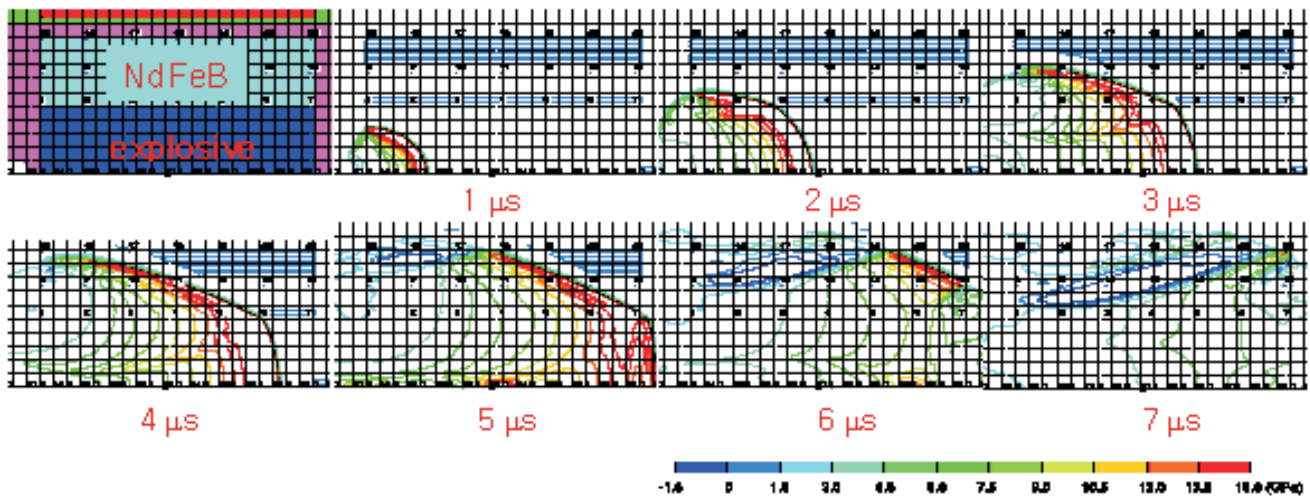


Fig. 10. Shockwave propagation in an annulus-type FMG.

of 25 GPa at the impact surface decreased down to 13 GPa, the assumed demagnetization pressure, after traveling about 0.5 mm at side, and 26 mm at the center. This result means that even the magnet of 20 mm in length was not magnetized completely. The decay in shock pressure occurred owing to expansion wave emerging from sides, which was proved by calculations for magnets of larger diameters that the decay occurred much slowly. This two dimensional effect negates the common belief that the plane shockwave is very important in FMG design, although the plane wave generator may alleviate the decay symptom only a little.

Based on these calculations, it could be said that, for the magnet of 60 mm in length, only a small part of the magnet was demagnetized, and, then, the considerable part of the generator coil acted as a load. This may explain the low energy output for the long magnets. The energy output from the magnets of 40 mm in length was still slightly higher than that from the magnets of 20 mm in length. This can happen only when considerable demagnetization occurred

below 13 GPa. Then, the increased demagnetization overcame the burden of inactive generator coil, and exerted more energy.

The energy output obtained from Tests C24 to C32 is plotted with respect to magnet volume in Figure 8. Results of Tests C1 to C14 were excluded in this plot because of long length compared to diameter. This Figure shows that the output energy is proportional to magnet volume if the ratio of length to diameter is kept less than 1.

Assuming constant flux density, the output energy can be shown to be proportional to the magnet volume by simple manipulation of equations, as follows [5]:

$$E \approx \frac{B^2 V}{8\mu K_L} \quad (3)$$

where E is output energy, V is magnet volume, μ is permeability of air, and K_L is a geometrical constant of generator coil. The output energy was expressed as a linear function of the magnet volume by using the

least squared error method, as is:

$$E = 0.0181V + 0.00027 \quad (4)$$

where E is given in J , and V in cm^3 . If the value of 0.27 J/cm^3 , the maximum energy of NdFeB listed in Table 1 is taken as a reference, the energy efficiency of the cylinder-type FMGs is estimated to be 6.7 %.

It should be noted that the ratio of length to diameter of a magnet has to be kept low, less than 1, for a cylinder-type FMG, to obtain maximum energy. For higher energy output, a magnet of larger diameter has to be used, or a new magnet of lower demagnetization pressure has to be employed.

3.4. Annulus-type FMGs

In the previous section, characteristics of the cylinder-type FMGs were discussed based on experiments and hydrodynamic calculations. The main disadvantages of the cylinder-type FMGs are the limitation in the ratio of length to diameter of magnets, and the use of shock generators. In order to obtain higher energy output, the diameter of a magnet has to be larger, and, as a result, more explosive has to be used in the shock generator, and, finally, the generator becomes very bulky. To overcome the above difficulty, the annulus-type FMGs were designed, as shown in Figure 2.

Eights tests were made for the Figure 4 while varying load characteristics, for cylinder-type FMGs, and their results are listed in Table 3. Typical voltage and current waveforms are shown in Figure 9. In this figure, the eddy current effect, which was discussed previously, was not present in the voltage waveform, at least apparently. This is because the shockwave moved somewhat perpendicularly, more precisely 35 degrees, to the flux in this type of FMG, not in the same direction with magnetic flux as in a cylinder-type FMG. In Figure 9, the voltage waveform shape was much different from that of a cylinder-type FMG, shown in Figure 4. In Table 2, the voltage for the annulus-type FMGs was measured to be much higher than that of the cylinder-type FMGs. As expected from Equation (2), the voltage is proportional to the rate of shocked volume. As can be seen in Figure 10, the volume of magnet shocked in a unit time was rather small initially, increased relatively gradually, reached to a maximum, and then, decreased relatively gradually. This is why the voltage waveform was much different from that of a cylinder-type FMG.

Figure 10 shows the shock propagation in an annulus-type FMG with a magnet of 50 mm in diameter and 40 mm in length. At approximately $2 \mu\text{s}$ after initiation of the explosive located at the center of the magnet, the shock wave entered into the magnet, and at $7 \mu\text{s}$ the shockwave reached at the upper right corner. The peak shock pressure was maintained over 13 GPa through the whole magnet, suggesting that

the efficiency of this type FMG should be higher than that of a cylinder-type FMG.

For the magnet of 50 mm in diameter and 40 mm in length, the output energy was estimated to be 1.5 J in Test A20, and the efficiency to be 9.4 %, which is 1.5 times higher than that of a cylinder-type FMG, 6.7 %. For the same magnet size but with a resistive load, the highest energy and efficiency were 1.75 J and 11 %, respectively in Test A17. In Test A17, the impedance of the resistive load was not matched to that of the generator coil, but the output energy was higher than that with a matched inductive load. This suggests that a FMG may work better with a resistive load than with an inductive load. In Test A22 in which the magnet length was doubled, 80 mm, the output energy was estimated to be 3.0 J, approximately twice higher than that with a magnet of 40 mm in length. In Test A23, the generator coil was divided into two 40 mm long coils connected in parallel. The output energy was the same with that for a 40 mm long magnet.

Although only a few experiments were made, the annulus-type FMGs exerted more energy with higher efficiency than the cylinder-type FMGs. The shock generator was not needed, and, consequently, the size was smaller, design was simpler, and the amount of explosive was smaller. Since there is no limit in magnet length to diameter, high energy output can be expected with large size. Because of these advantages, the annulus-type FMGs are one of the best candidates for an autonomous pulsed power supply.

4. Conclusions

Output characteristics of the cylinder- and annulus-types of explosively-driven FMGs based on NdFeB magnets were investigated experimentally while varying design features. Extensive hydrodynamic calculations were made to explain experimental findings. The conclusions of this study are the followings:

1. For the cylinder-type FMGs, the ratio of magnet length to diameter has to be kept low, less than 1, to obtain high energy efficiency. The highest energy efficiency obtained in experiments was estimated to be 6.7 % with respect to the maximum magnetic energy stored in the magnet.
2. The annulus-type FMGs showed better performance than the cylinder-type FMGs; higher energy and efficiency. The highest efficiency for this type of FMGs was 9.4 % with a matched inductive load, and 11% resistive load.
3. In addition to higher energy efficiency, the annulus-type generators have many advantages over the cylinder-type FMGs; simple design, smaller size, and no size limitation. Because of

these advantages, the annulus-type FMGs can be regarded as the most viable autonomous pulsed power supply for many applications.

Manuscript received August 1, 2003

[9] Dobratz N.M. and Crawford P.C. LLNL explosives handbook: Properties of chemical explosives and explosive simulants // Lawrence Livermore Technical Lab., Livermore, CA, Tech. Rep. UCRL-52997-Chg. 2, Jan. 1985.

References

- [1] Kristiansen M. Fundamental limits to compact expendable pulsed power and microwave sources // in Progress Report on Explosives Test: – Nov. 29-Dec. 2, 1999.
Available: <http://ppl.ee.ttu.edu>, Directory: projects/expandable/pulsed/power, File: reporttext99.
- [2] Shkuratov S.I., Talantsev E.F., Dickens J.C. and Kristiansen M. Transverse shock wave demagnetization of NdFeB high-energy hard ferromagnetics // J. Appl. Phys. – 2002. – V. 92. – P. 3007–3009.
- [3] Shkuratov S.I., Talantsev E.F., Dickens J.C. and Kristiansen M. Ultracompact explosively-driven high-current source of primary power based on shock wave demagnetization of NdFeB high-energy hard ferromagnetics // Rev. Sci. Instrum. – 2002. – V. 73. – P. 2738–2742.
- [4] Lee J., Choi J.S., Yim D.W. and Ahn J.W. Output characteristics of explosively-driven ferromagnetic generators // Proceedings of the 13-th IEEE International Pulsed Power Conference. – Las Vegas, NV. – June 17–22, 2001. – P. 154–157.
- [5] Choi J.S., Lee J., Ryu J.H., and Ahn J.W. Explosively- Driven Ferromagnetic Generators as an Initial Energy Source of Compact Pulsed Power Systems // presented in 2002 American Electromagnetic Symposium. – Annapolis, USA. – June 2002.
- [6] Royce E.B. Properties of magnetic materials under shock compression, in Physics of high energy density, Keeler R.N. and Royce E.B. – New York: Academic Press. – 1974. – P. 126–138.
- [7] Kaufman L. Phase equilibria and transformations in metals in Solids under pressure Paul W. and Warschauer D.M. – New York: Mcraw-Hill. – 1963. – P. 304–356.
- [8] Graham R.A. Pressure dependence of the magnetization of Invar and Silectron from 30-450 kbar // J. Appl. Phys. – 1968. – V. 19. – P. 437–439.